ISSN: 2641-2039
DOI: 10.33552/GJES.2020.06.000646
Global Journal of Engineering Sciences
Iris Publishers

Research Article

A DFT study of the Optoelectronic properties of $Sn_{1-x}A_xS$ (A= Au and Ag) Solar Cell Applications

Zeesham Abbas[1]*, Nawishta Jabeen[1], Sikander Azam[2], Muhammad Asad Khan[1] and Ahmad Hussain[1]*

[1]*Department of Physics, The University of Lahore, Sargodha campus, 40100 Sargodha, Pakistan*

[2]*Faculty of Engineering and Applied Sciences, Department of Physics, RIPHAH International University I-14 Campus, Islamabad, Pakistan*

***Corresponding author:** Ahmad Hussain and Zeesham Abbas, Department of Physics, The University of Lahore, Sargodha campus, 40100 Sargodha, Pakistan.

Received Date: November 19, 2020

Published Date: December 01, 2020

Abstract

Doping effect of transition metal (TM) atoms on the photovoltaic features of Sn1-xAxS (A= Au and Ag) is investigated theoretically. DFT based calculations are used to explore electronic and optical properties by using full potential linearized augmented plane wave (FP-LAPW) method. Furthermore, generalized gradient (GGA) approximation is applied for the treatment of exchange and correlation potential. Ground state properties of these compounds are calculated by using GGA approximation. Our investigation shows that these compounds are metallic in nature. Origin of atomic/orbital electronic states in the energy band dispersion are explored in detail for S, Sn, Au and Ag from the calculated spectra of density of states. Optical parameters like complex dielectric function are also evaluated by using the information of energy band dispersions along with other associated optical properties like refractive index, optical conductivity, extinction coefficient, absorption coefficient, energy loss function and reflectivity coefficient. This study confirms that these TM based compounds can be used as promising compounds for technological optoelectronic applications having desired properties.

Introduction

In recent years, researchers have developed their interests in intermediate band (IB) materials due to their technological application is solar cells [1]. In next generation solar cells, the problem of efficiency can be overcome by developing IB photovoltaic materials. The working demonstration of intermediate solar cells is shown in Figure 1.

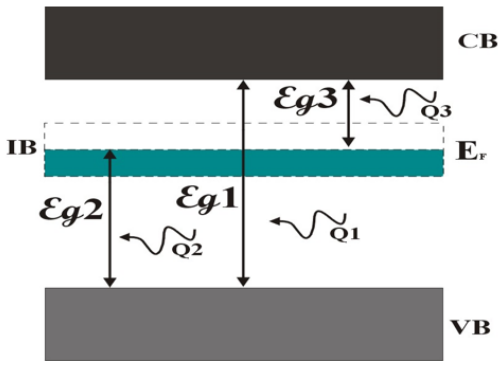

Figure 1: Working demonstration of intermediate band solar cell [2].

Arrows in the diagram show the possible electronic transitions. These electronic transitions can also take place in traditional way from valance band (VB) to conduction band (CB). In above figure, energy gaps between IB-CB, VB-IB and VB-CB are represented by *Eg3*, *Eg2* and *Eg1*, respectively, and Fermi level is specified by E_F. It can also be noted that IB can offer accommodation for the electrons travelling from VB to CB with less energy as compared to Eg1. Electrons can move from VB to IB and then from IB to CB in the materi als possessing IB. Several features of solar cells based on IB materials are presented in Figure 1. Existence of an isolated IB at Fermi level is the most prominent among all feature. Thermal relaxations can be produced due to interaction of electrons and the phonons of crystal lattice if this condition is not satisfied [2]. Moreover, IB must have a specified thickness so that the phenomenon of non-radiative recombination be avoided as much as possible. Electrons coming from VB with lower energies as compared to the energy difference between VB and CB can stay in IB only if it is partially filled.

Solar cells with this construction have higher conversion efficiencies then those established by Shockley limit [3], as reported earlier by Luque and Marti [1]. They reported the increase in the efficiency of these solar cells by operation and thermodynamic arguments. Diluted oxides with II-VI composition [4] or quantum dots can be introduced in the geometry [5] to prepare materials having IB.

Main focus of this investigation is the study of optical and electronic properties of $Sn_{1-x}A_xS$ (A= Au and Ag) having IB with the help of quantum mechanical methodology. Additionally, electronic and optical properties of aforesaid compounds can also be calculated by using this methodology. We will discuss methodology and then investigated results will be discussed in the successive parts.

Methodology

Kohn-Sham equations are solved in order to calculate ground state properties of $Sn_{1-x}A_xS$ (A= Au and Ag) by using self-consistent approach with the help of full potential linearized augmented plane wave (FP-LAPW) method [6] within the framework of DFT [7,8] as executed in WIEN2K code [9,10]. Exchange and correlation energy (E_{xc}) were treated by using GGA approximation while calculating optical and electronic properties of $Sn_{1-x}A_xS$ (A= Au and Ag). Optimized geometric structure was achieved through minimization of forces from the atoms of unit cell to carry out this DFT study.

Muffin-tin spheres and the interstitial region (IR) are the two main parts of the crystal unit cell while working with FP-LAPW method. Here, core and valance electrons are treated as two separate groups of the electrons. In this technique, muffin-tin (MT) model is used to drive crystal potential. Valance electrons and non-overlapping atomic spheres with radius R_{MT} (smallest muffin-tin radius) are termed as IR and muffin-tin spheres. The product of Spherical harmonics (Y_{lm}) and radial solution of Schrodinger wave equation (SWE) at fixed energy for single particle (V_{lm}) is used to specify potential in muffin-tin spheres.

$$V(r) = \Sigma_{l,m} V_{lm}(r) Y_{lm}(r) \qquad (1)$$

On the other hand, the following expression can be used to expand wave function in IR of the crystal unit cell by using plane wave basis set [11]:

$$V(r) = \Sigma_k V_k e^{i\vec{k}.\vec{r}} \qquad (2)$$

A k-mesh of 500 k-points, l_{max} =10 (maximum value of angular momentum) and the value of $R_{MT}k_{max}$ = 7 (k_{max} and R_{MT} are cut-of wave vector of the plane wave basis and smallest value of muffin-tin radius, respectively) was choose to perform these calculations. Step size of the charge density is taken as 0.00001e a_0^{-3} for termination of the iterations, also known as convergence criterion Valance and core states are separated by -8 Ry (core cut-off energy). Crystalline structures of $Sn_{1-x}A_xS$ (A= Au, Ag) are shown in Figure 2.

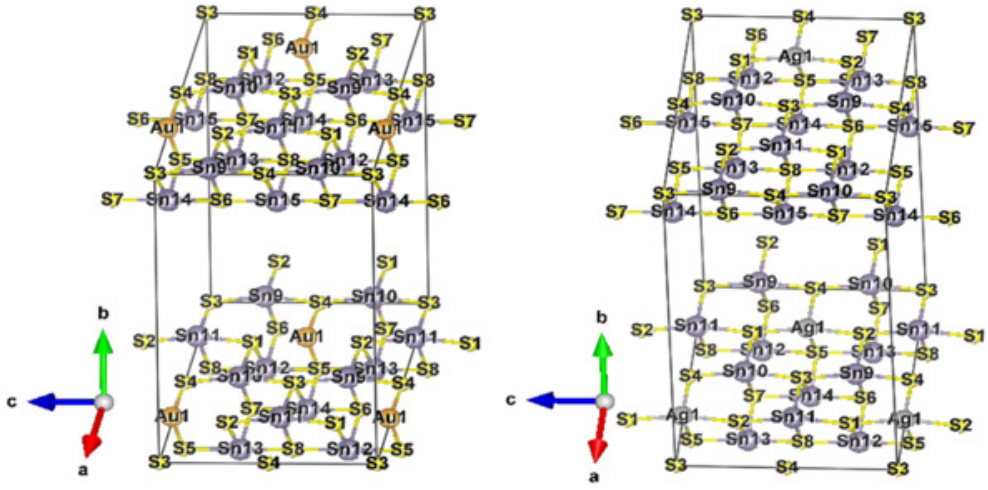

Figure 2: Crystalline structures of $Sn_{1-x}A_xS$ (A= Au, Ag).

Results and Discussion

Electronic properties

In this section, we have presented the electronic properties of $Sn_{1-x}A_xS$ (A= Au, Ag) namely the energy band structures and the density of states. Energy band structures are presented along highly symmetric points of Brillouin zone for a continuous energy range of -5.0 to 5.0 eV. Density of states are presented for a continuous energy range of -6.0 to 6.0 eV to determine the possible electronic transitions from CB to VB.

Band structure

In this section, energy band structures for the supercells of $Sn_{1-x}A_xS$ (A= Au, Ag) are discussed along highly symmetric points of the irreducible Brillouin zone (IBZ). Calculated structures are shown in Figure 3 by setting Fermi level at 0 eV. An entirely isolated extra band can be seen at Fermi level of both the band structures of $Sn_{1-x}A_xS$ (A= Au, Ag) known as intermediate band (IB). We can see that this band cross Fermi level. Intermediate bands can be divided into three types depending on the number of electrons in the IB as type I, type II and type III as shown in Figure 4. Type I and III are completely empty and they can be used to store electronic charge in the form of holes and electrons [12]. In literature, we can find several materials that carry IB for Li-ion batteries such as $LiMn_2O_4$, $LiCoO_2$ etc [13]. $Sn_{1-x}A_xS$ (A= Au, Ag) are potential candidates for technological applications in solar cells due to their partially filled IB. Materials with type-II IB are the main focus of this study. We can observe that energy band gap is present between IB and CB. This band gap decreases as we use Au as dopant instead of Ag. Energy band gap between IB and CB is approximately 1.0 and 1.5 eV for $Sn_{1-x}Au_xS$ and $Sn_{1-x}Ag_xS$, respectively.

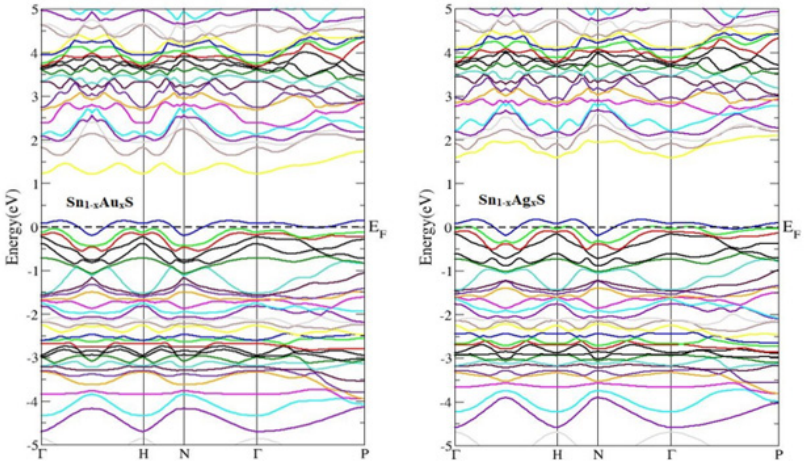

Figure 3: Electronic band dispersions for $Sn_{1-x}A_xS$ (A= Au, Ag). .

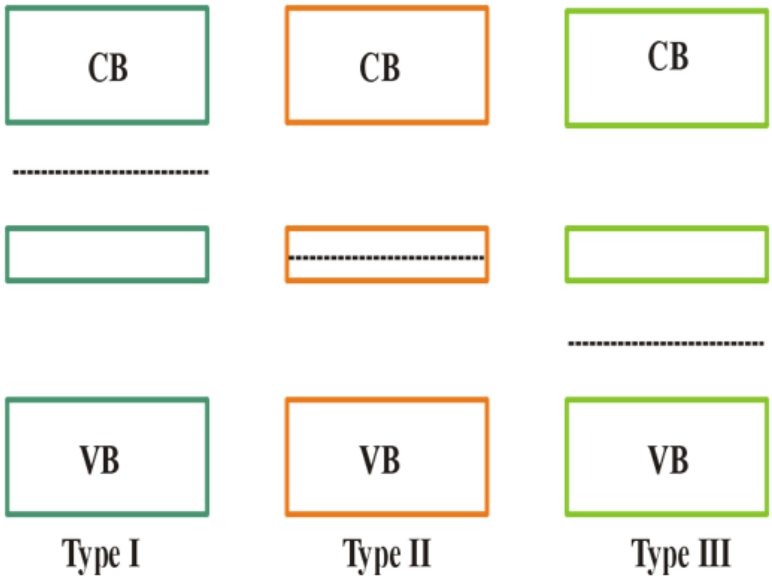

Figure 4: Types of intermediate band w.r.t. position of Fermi level.

Density of states

Partial (PDOS) and total density states (TDOS) are calculated to get insight of the possible electronic transitions and their impact on various ground state properties. Calculated spectra of DOS for $Sn_{1-x}Au_xS$ and $Sn_{1-x}A_xS$ are presented in Figure 5 and Figure 6, respectively. We can observe from Figure 5 that Au-atoms have key impact in the valance band of $Sn_{1-x}Au_xS$, however, minor impact of S and Sn-atoms is also present. An IB due to hybridization of Au-d and S-p orbitals is also present around Fermi level. In conduction band, we can observe that S and Sn-atoms have key impact, however, minor impact of Au-atoms is also present.

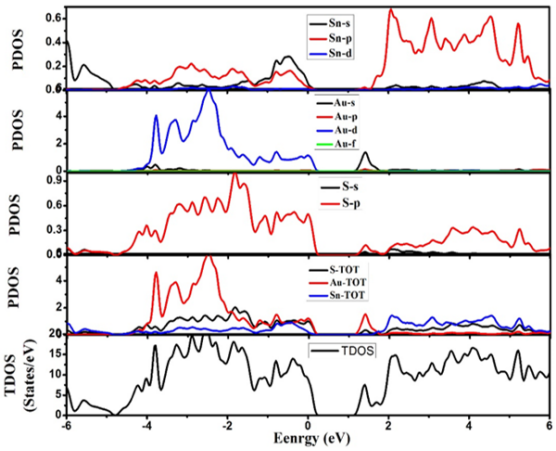

Figure 5: Total and partial density of states for Sn1-xAuxS.

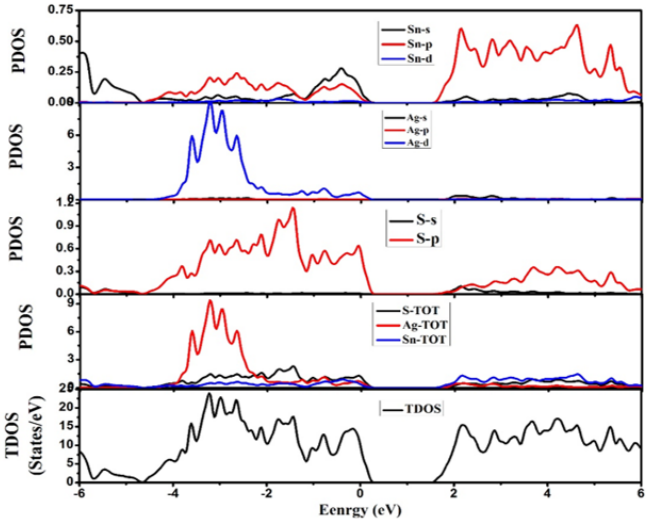

Figure 6: Total and partial density of states for Sn1-xAgxS.

From the spectra of PDOS, we can note that VB can be divided into three parts as part A (-6.0 to -4.0 eV), part B (-4.0 to -2.0 eV) and part C (-2.0 to 0 eV). In part A, possible electronic transitions occur only due Sn[$5s^2$] orbitals because all other orbitals are silent in this region. In part B, major electronic contributions come from Sn[$5p^2$], Au[$5d^{10}$] and S[$3p^4$]. Finally, in part C of the VB, major electronic contributions come from Sn[$5p^2$], Sn[$5s^2$], Au[$5d^{10}$] and S[$3p^4$]. From the spectra of PDOS, we can note that S[$3p^4$] and Sn[$5p^2$] orbitals have key impact in CB, however, minor impact of Au[$6S^1$] is also present.

We can observe from Figure 6 that Ag-atoms have key impact in the central part of valance band of $Sn_{1-x}Au_xS$, however, minor impact of S and Sn-atoms is also present. An IB due to hybridization of Ag-d and S-p orbital is also present around Fermi level. In conduction band, we can observe that S and Sn-atoms have key impact, however, minor impact of Ag-atoms is also present [12,13].

From the spectra of PDOS, we can note that VB can be divided into three parts as part A (-6.0 to -4.0 eV), part B (-4.0 to -2.0 eV) and part C (-2.0 to 0 eV). In part A, possible electronic transitions occur only due Sn[$5s^2$] orbitals because all other orbitals are silent in this region. In part B, major electronic contributions come from Sn[$5p^2$], Ag[$4d^{10}$] and S[$3p^4$]. Finally, in part C of the VB, major electronic contributions come from Sn[$5p^2$], Sn[$5s^2$], Ag[$4d^{10}$] and S[$3p^4$]. From the spectra of PDOS, we can note that S[$3p^4$] and

Sn[5p^2] orbitals have key impact in CB, however, minor impact of Ag[5S^1] is also present.

Fermi surface

Due to metallic nature of $Sn_{1-x}A_xS$ (A= Au, Ag), Fermi surfaces (FS) are also investigated for the accessible electronic states of these compounds. Configuration of near Fermi bands present in $Sn_{1-x}A_xS$ (A= Au, Ag) are shown in Figure 7 for the highly symmetric points of IBZ. Electrons near Fermi level play an important role in the electronic conductivity of the material. Understanding of the electronic properties of metallic compounds (band structure and DOS) can be obtained from their FS. Comprehensive knowledge of the electronic states (at Fermi level (E_F)) can be obtained from FS. Electronic sheets and holes in the FS are represented by colored region and the empty spaces, respectively. Maximum region of the FS is empty for both compounds which show that these compounds are p-type semiconductors. From band structure, we can note that there is only one band that cross E_F in both compounds. Thermoelectric properties such as electrical conductivity is directly related to the topography of the FS. Electrons with various velocities are represented by different colors in the FS.

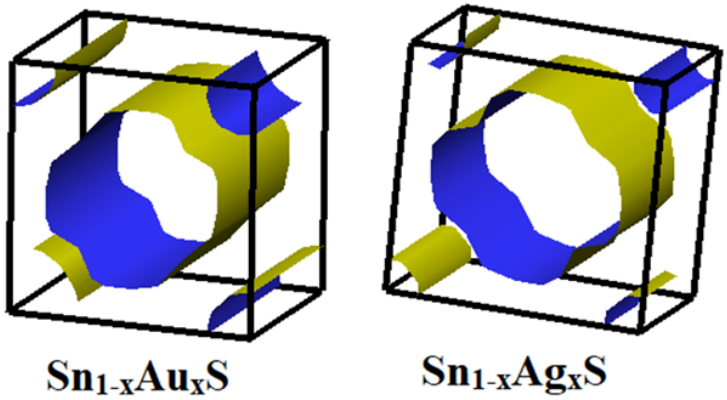

Figure 7: Fermi surfaces for Sn1-xAxS (A= Au, Ag).

Optical properties

In this section of the manuscript, optical properties of $Sn_{1-x}A_xS$ (A= Au, Ag) are discussed in order to investigate usability of aforesaid compounds in various industries like optoelectronics, solar cells and telecommunication. Dielectric constant ε(ω), refractive index n(ω), extinction coefficient k(ω), reflectivity R(ω), absorption coefficient I(ω), energy loss function L(ω) and optical conductivity σ(ω) are calculated with the help of following expressions [14,15].

$$\varepsilon_1(\omega) = 1 + \frac{2}{\pi} P\int_0^{\infty} \frac{\omega^{'}\varepsilon_2(\omega')}{\omega^{'2} - \omega^2} d\omega^{'} \qquad (3)$$

$$\varepsilon_1(\omega) = \frac{e^2 h'}{\pi m^2 \omega^2} \sum_{v,c} \int_{BZ}^{\infty} \left|M_{cv}(k)\right|^2 \delta\left[\omega_{cv}(k) - \omega\right] d^3k \qquad (4)$$

$$n(\omega) = \left[\frac{\varepsilon_1(\omega)}{2} + \frac{\sqrt{\varepsilon_1^2(\omega) + \varepsilon_2^2(\omega)}}{2}\right]^{\frac{1}{2}} \qquad (5)$$

$$k(\omega) = \left[-\frac{\varepsilon_1(\omega)}{2} + \frac{\sqrt{\varepsilon_1^2(\omega) + \varepsilon_2^2(\omega)}}{2}\right]^{\frac{1}{2}} \qquad (6)$$

$$k(\omega) = \frac{(n-1)^2 + k^2}{(n+1)^2 + k^2} \qquad (7)$$

$$\alpha(\omega) = \frac{4\pi k(\omega)}{\lambda} \qquad (8)$$

$$\sigma(\omega) = \frac{2W_{cv} h' \omega}{E_0} \qquad (9)$$

$$\sigma(\omega) = \mathrm{Im}\left(-\frac{1}{\tilde{\varepsilon}(\omega)}\right) \qquad (10)$$

Where W_{cv} represents transition rate per unit time. Nature of interaction between the aforesaid compounds and incident photons can also be discussed by using complex dielectric function ε(ω). Information regarding the polarization of the investigated material in the presence of external field is obtained from ε(ω). There are three major components of ε(ω) i.e. $\varepsilon^{xx}(\omega)=\varepsilon^{yy}(\omega)$ and $\varepsilon^{zz}(\omega)$ because $Sn_{1-x}A_xS$ (A= Au, Ag) belongs to tetragonal crystal system but we have plotted the average of these components for all optical parameters. Complex dielectric function ε(ω) can be calculated by using following expression [16].

$$\varepsilon(\omega) = \varepsilon^1(\omega) + i\varepsilon^2(\omega) \qquad (11)$$

Where real and imaginary part of complex dielectric function ε(ω) are represented by $\varepsilon_1(\omega)$ and $\varepsilon_2(\omega)$, respectively. Photon dispersion can be explained by $\varepsilon_1(\omega)$ due to interaction of host com-

pound and the incident photons. It is used to discuss interbond electronic transitions due to the absorption of incident photons. Kramer-Kronig expression can be used to associate these parameters with other optical parameters [17,18]. All optical parameters are calculated over a continuous energy range of 0 to 14 eV.

Real part ε_1 (ω) of complex dielectric function over an entire energy range of 0 to 14 eV is shown in Figure 8(a). Major peaks of ε_1 (ω) are present in visible and infrared region. After 2.5 eV, curves for both materials start decreasing and enters the negative region at approximately 5.5 eV. These negative values of ε_1(ω) corresponds to the metal like reflecting nature of $Sn_{1-x}A_xS$ (A= Au, Ag). Zero frequency limit (static values) of ε_1(0) can also be determined with the help of calculated spectra of ε_1(ω). Estimated values of ε_1(0) are appeared to be 14.3 and 14.2 for $Sn_{1-x}Au_xS$ and $Sn_{1-x}Ag_xS$, respectively. Energy band gap E_g and ε_1(0) are inversely related to each other. Following expression of the Penn's model can be used to relate E_g and ε_1(0) [19].

$$\varepsilon_1(0) \approx 1 + \left(\frac{\hbar\omega p}{E_g}\right)^2 \quad (12)$$

Imaginary part ε_2 (ω) of complex dielectric function over an entire energy range of 0 to 14 eV is shown in Figure 8(b). Major peaks of ε_2 (ω) are present in infrared region of the optical spectrum. In the spectra of ε_2 (ω), a unique property is its critical value. Absorption and transmission of incident photons occur above and below threshold energy of $Sn_{1-x}A_xS$ (A= Au, Ag), respectively. No transmission of photons is present in $Sn_{1-x}A_xS$ (A= Au, Ag) as their threshold energy is below 0 eV, so, all the incident photons are absorbed by these materials. Prominent peaks are present at approximately 0.5 eV and then at approximately 6.0 eV for both compounds in the spectra of ε_2 (ω). Some peaks are also present in visible region between 1.7 and 3.1 eV.

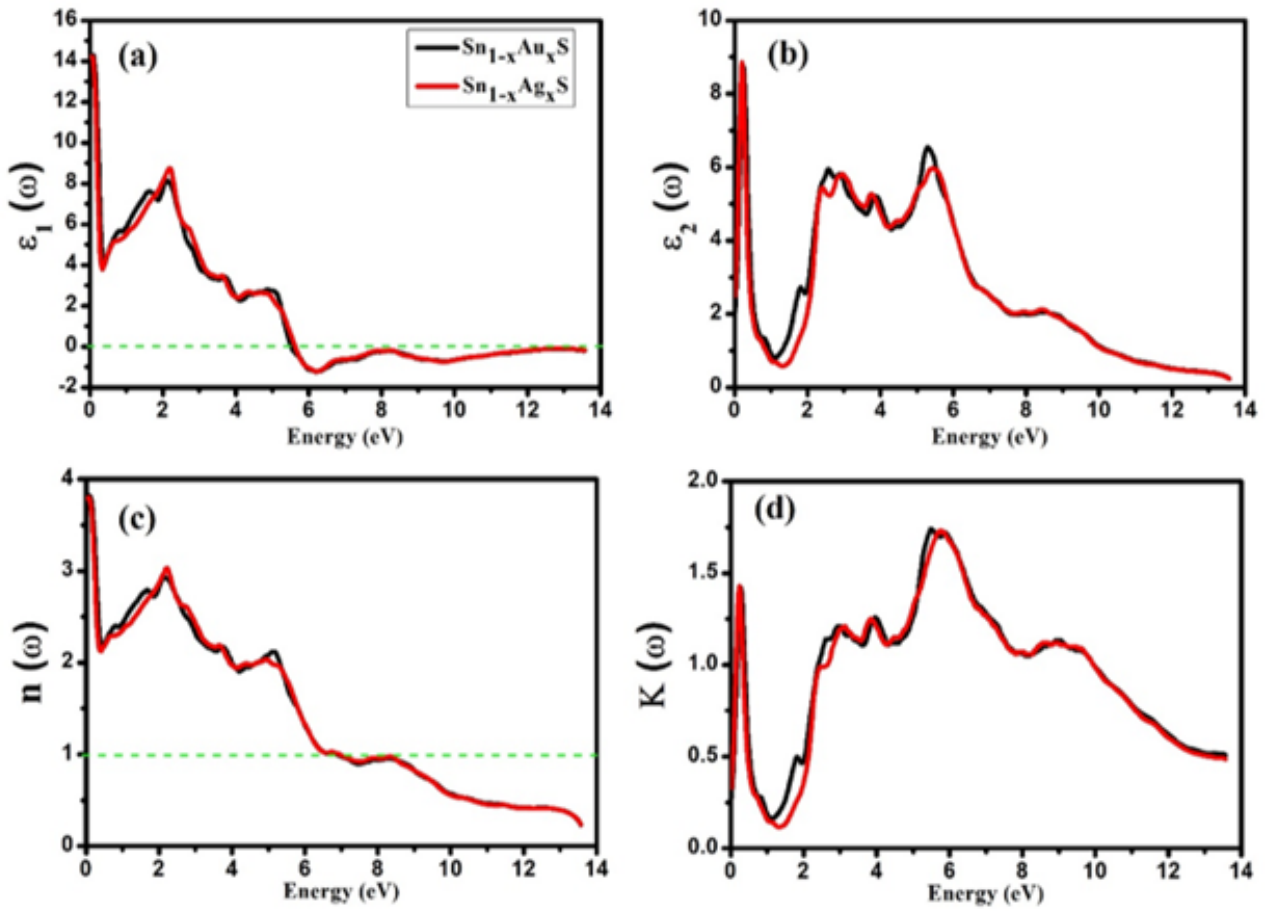

Figure 8: Calculated (a) Real part ε1 (ω) (b) imaginary part ε2 (ω) of complex dielectric function (c) Refractive index n(ω) and (d) extinction coefficient k(ω) for Sn1-xAxS (A= Au, Ag).

Refractive index n(ω) and extinction coefficient k(ω) calculated for $Sn_{1-x}A_xS$ (A= Au, Ag) are shown in Figure 8(c) and 8(d), respectively, over an entire energy range of 0 to 14 eV. Calculated values of ε_1 (ω) and ε_2 (ω) can be used to calculate n(ω) and k(ω) with the help of following expressions:

$$\varepsilon_1(\omega) = n^2 - k^2 \qquad (13)$$

$$\varepsilon_1(\omega) = 2nk \qquad (14)$$

Refractive index n(ω) can be used to discuss transparency and dispersion behavior of the compounds. Major peaks of n(ω) are present in visible and infrared region. After 2.5 eV, curves for both materials start decreasing and becomes less that unity at approximately 7.0 eV. It shows that photons with these energies are opposed by the polarization of aforesaid compounds because speed of light become less than the group velocity (V_g=c/n) [20]. Zero frequency limit (static values) of n(0) can also be determined with the help of calculated spectra of n(ω). Estimated values of n(0) are appear to be 3.79 for both $Sn_{1-x}Au_xS$ and $Sn_{1-x}Ag_xS$. Energy band gap E_g and ε_1 (0) are inversely related to each other. Following expression of the Penn's model can be used to relate n(0) and ε_1 (0).

$$n(0)=\sqrt{\varepsilon_1(0)} \qquad (15)$$

Extinction coefficient k(ω) can be used to explain the features similar to that of ε_2 (ω) like absorption of light. Major peaks of k(ω) are present in ultraviolet region of the optical spectrum. In the spectra of k(ω), a unique property is its critical value. No transmission of photons is present in $Sn_{1-x}A_xS$ (A= Au, Ag) as their threshold energy is below 0 eV, so, all the incident photons are absorbed by these materials. Prominent peaks are present at approximately 0.5 eV and then at approximately 6.0 eV for both compounds in the spectra of k(ω). Some peaks are also present in visible region between 1.7 and 3.1 eV.

Reflectivity R(ω) and energy loss function L(ω) calculated for $Sn_{1-x}A_xS$ (A= Au, Ag) are shown in Figure 9(a) and 9(b), respectively, over an entire energy range of 0 to 14 eV. Surface study of $Sn_{1-x}A_xS$ (A= Au, Ag) is also discussed by calculating the difference of the reflected power and incident power known as reflectivity R(ω). Zero frequency limit (static values) of R(0) can also be determined with the help of calculated spectra of R(ω). Estimated values of R(0) are appear to be 0.341 and 0.342 both $Sn_{1-x}A_xS$ and $Sn_{1-x}A_xS$, respectively. Behavior of R(ω) and ε_1 (ω) is similar to each other. Hence, R(ω) and absorption coefficient I(ω) are inversely related to each other which implies that I(ω) will be lower in the region where the values of R(ω) are higher and vice versa. Various peaks are present in the spectra of R(ω) because of anisotropy of the material. However, R(ω) show its maximum peak in UV region where ε_1 (ω) is negligible because in this region energy gap is zero and material reflects almost all the incident photons due to its reflecting metallic nature.

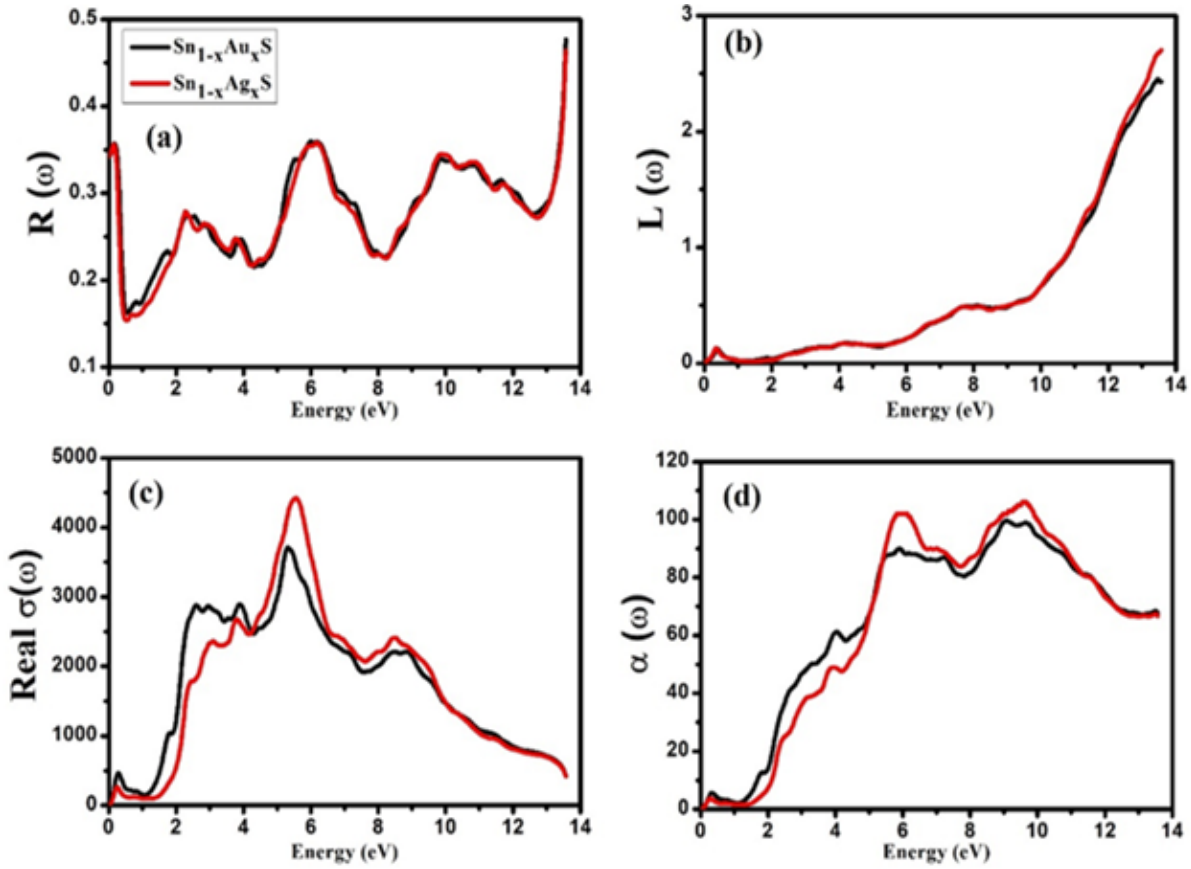

Figure 9: (a) Reflectivity R(ω), (b) energy loss function L(ω), (c) optical conductivity σ(ω) and absorption coefficient I(ω) for Sn1-xAxS (A= Au, Ag).

Loss of rapidly moving electrons in the material can be explained by an important optical parameter known as energy loss function L(ω). Plasma oscillations are responsible for the characteristic behavior of the peaks present in the spectra of L(ω) and the frequencies associated with these oscillations are known as plasma frequencies. Plasmon excitations are responsible for the major peaks in the calculated spectra of L(ω). It is due to the mutual oscillations of the background atomic cores against the valance electrons in the longitudinal fashion with plasma frequency ω_p. We can note from the spectra of L(ω) that there is negligible loss of electron energy up to 10.0 eV and then the spectra of L(ω) becomes maximum in upper UV region [17-20].

Optical conductivity σ(ω) and absorption coefficient α(ω) calculated for $Sn_{1-x}A_xS$ (A= Au, Ag) are shown in Figure 9(c) and 9(d), respectively, over an entire energy range of 0 to 14 eV. Measure of the produced charge carriers due to breaking of the bond of atoms in the material due to incident photons which gives reasonable forward current is presented by σ(ω). Highest peaks of σ(ω) are present between 2.0 to 8.0 eV. We can note from the variations of σ(ω) show similar behavior as that of α(ω), k(ω) and ε_2 (ω). Absorption of incident photons by the host materials is responsible for this behavior of σ(ω).

Information regarding penetration length of the incident photons inside the host material is given by absorption coefficient α(ω). Absorption coefficient α(ω) can be calculated by using the following expression [21]:

$$\alpha(\omega)=\sqrt{2}\omega\left[\sqrt{\varepsilon_1(\omega)^2+\varepsilon_2(\omega)^2}-\varepsilon_1(\omega)\right]^{\frac{1}{2}}$$

Both materials show no absorption of incident photons till 1.5 eV, inside the outlawed energy band. Because of electronic transitions from VB to CB, we can note prominent peaks in the spectra of α(ω) between 5.0 to 11.0 eV.

Conclusion

GGA potential scheme is used with DFT based FP-LAPW approach to explore the effect of TM atoms on ground state properties of $Sn_{1-x}A_xS$ (A= Au, Ag). Electronic properties show that these compounds are metallic in nature. GGA functional is employed to calculate band structures and DOS (total and partial) in order to get accurate knowledge of the electronic properties. Our calculations show that these compounds possess intermediate band and energy band gap (between IB and CB) of these materials decreases as we change dopant from Ag to Au. We conclude that these materials are p-type semiconductors above IB. Optical parameters for $Sn_{1-x}A_xS$ (A= Au, Ag) are also calculated to get insights of the usability of these compounds in technological optical applications. We conclude that these materials are not good reflectors as they reflect maximum of 50 % of the incident photons in upper UV region.

Acknowledgement

The work is supported by the Higher Education Commission of Pakistan start-up research grants No: 21-2344/SRGP/R&D/HEC/2019 and 21-2340/SRGP/R&D/HEC/2019.

Conflict of Interest

No conflict of interest.

References

1. A Luque, A Marti (1997) Phys Rev Lett 78: 5014.
2. Abbas Z, Munaf S, Azam S, Abubakar M, Irfan M (2020) First-principles Calculations of Optoelectronic Properties of Sn1-xInxA (A= S and Se) for Solar Cell Applications (No. 2748).
3. W Shockley, HJ Queisser (1961) J Appl Phys 32: 510.
4. A Marti, L Cuadra, A Luque (2000) Proceedings of the 28th IEEE Photovoltaics Specialists Conference, vol. 940, IEEE, New York.
5. KM Yu, W Walukiewicz, J Wu, W Shan, JW Beeman, et al. (2003) Phys Rev Lett 91(24): 246403-1.
6. OK Andersen (1975) Phys Rev B 42: 3063-3083.
7. P Hohenberg, W Kohn (1964) Phys Rev B 136: 864-871.
8. W Kohn, LJ Sham (1965) Phys Rev 140: A1133-A1138.
9. P Blaha, K Schwarz, P Sorantin, SK Trickey (1990) Comput Phys Commun 59: 339-415.
10. P Blaha, K Schwarz, GH Madsen, D Kvasnicka, J Luitz (2001) WIEN2k, an Augmented Plane Wave Plus Local Orbitals Program for Calculating Crystal Properties, Vienna University of Technology Vienna, Austria.
11. Azam S, Irfan M, Abbas Z, Rani M, Saleem T, et al. (2019) DFT study of the electronic and optical properties of ternary chalcogenides AlX2Te4. Materials Research Express 6(11): 116314.
12. ACM Padilha, H Raebiger, AR Rocha, GM Dalpian (2016) Charge storage in oxygen deficient phases of TiO_2: defect Physics without defects. Sci Rep 6: 28871.
13. EG Ladopoulos, D Str (2017) Stationary energy storage by next generation lithium – ion batteries with intermediate bands. Univ J Computat Anal 5: 12-19.
14. FK Butt, AS Bandarenka (2016) Microwave-assisted synthesis of functional electrode materials for energy applications. J Solid Stat Electro chem 20: 2915–2928.
15. Q Mahmood, M Yaseen, M Hassan Asif Mahmood (2017) Chin Phys B 26(8): 087803.
16. Azam S, Irfan M, Abbas Z, Khan SA, Khenata R, et al. (2020) Optoelectronic properties of Nd3+ doped CaTa2O6: Insights from the GGA+ U calculations. Optik.
17. E Schreiber, OL Anderson, N Soga (1973) Elastic Constants and Their Measurements, first ed., McGraw-Hill, New York.
18. F Wooten (1972) Optical Properties of Solids, Academic Press, New York.
19. DR Penn (1962) Phys Rev 128: 2093.
20. K Xiong, J Robertson, SJ Clark (2006) Appl Phys Lett 89: 022907.
21. Sonali Saha, TP Sinha, Abhijit Mookerjee (2000) Phys Rev B 62: 8828.